Postprint of: Nosko O., Thermal boundary conditions to simulate friction layers and coatings at sliding contacts, International Journal of Heat and Mass Transfer, Vol. 127, Part A (2018), pp. 1128-1137, DOI: 10.1016/j.ijheatmasstransfer.2018.06.027

Thermal boundary conditions to simulate friction layers and coatings at sliding contacts

Oleksii Nosko

Bialystok University of Technology, Faculty of Mechanical Engineering,
ul. Wiejska 45C, Bialystok, 15-351, Poland
E-mail: o.nosko@pb.edu.pl

A brief review of the thermal boundary conditions specified at sliding interfaces was performed. New thermal boundary conditions were derived aimed at solving problems of sliding with account of surface layers representing friction layers and tribological coatings. Based on the assumption of linear temperature distributions in the surface layers, the proposed conditions enable one to simplify simulations by eliminating the surface layers from consideration and merging thermally the bulk bodies. A problem of non-stationary heat conduction in two sliding semispaces with the proposed conditions at their interface was solved analytically. The particular cases of the solution were shown to coincide with the exact temperature expressions obtained for different well-known boundary conditions. The temperature influence of the basic parameters was analysed in dimensionless form on example of a decelerative sliding between a semispace covered with a surface layer and a semispace of constant temperature. An estimation of the error introduced by the proposed conditions was done. It was found that the error is below 1% for a wide class of friction layers and coatings met in practice.

Keywords: thermal boundary conditions, thermal friction contact, imperfect thermal contact, sliding interface, friction layer, tribological coating.

Notation

c	surface layer heat capacity, $c = K_\mathrm{s} h / k_\mathrm{s}$	Fo	dimensionless time variable, $\mathrm{Fo} = kt/h^2$
c_i	ith surface layer heat capacity, $c_i = K_{si} h_i / k_{si}$	Fo_0	dimensionless sliding duration, $\mathrm{Fo}_0 = kt_0/h^2$
e_i	ith body thermal effusivity, $e_i = K_i/\sqrt{k_i}$	K	body thermal conductivity
h	surface layer thickness	K_i	ith body thermal conductivity
h_c	contact heat transfer coefficient	K_s	surface layer thermal conductivity
h_i	ith surface layer thickness	K_{si}	ith surface layer thermal conductivity
i	body number, $i \in \{1,2\}$	Q	dimensionless power of heat generation, $Q = \alpha q / q_0$
j	imaginary unit	T	body temperature
k	body thermal diffusivity	T_i	ith body temperature
k_i	ith body thermal diffusivity	α	heat-generation coefficient
k_s	surface layer thermal diffusivity	α_f	heat-partition coefficient
k_{si}	ith surface layer thermal diffusivity	γ	roughness contact heat transfer coefficient
q	specific power of heat generation	ε	boundary condition percent error
q_0	initial specific power of heat generation	ϑ	dimensionless temperature, $\vartheta = KT/(q_0 h)$
r	surface layer thermal resistance, $r = h/K_\mathrm{s}$	ϑ_max	maximum dimensionless temperature, $\vartheta_\mathrm{max} = \max\{\vartheta\}\vert_{\xi=0,\ 0<\mathrm{Fo}\le\mathrm{Fo}_0}$
r_i	ith surface layer thermal resistance, $r_i = h_i/K_{si}$	ξ	dimensionless spatial coordinate, $\xi = x/h$
s	Laplace transform parameter	π	Pi number
t	time variable	χ	thermal diffusivity ratio, $\chi = k_\mathrm{s}/k$
t_0	sliding duration	Λ	thermal conductivity ratio, $\Lambda = K_\mathrm{s}/K$
x	spatial coordinate	$\mathcal{L}$	Laplace transform operator
B	dimensionless contact heat transfer coefficient, $B = \gamma h/K$	$\tilde{\blacksquare}$	Laplace transform image

1. Introduction

In Tribology, Contact Mechanics, and other branches of natural science investigating interactions between different media, problem statement accuracy is crucially dependent on the type of boundary conditions specified at the interface. The development of the boundary conditions used currently for simulating thermal processes at static and sliding contacts has a long history, stemming from the formulation of the heat-conduction equation by Fourier [1].

Carslaw [2] (p.161, 214) derived analytical solutions of heat-conduction problems for two coupled bodies assuming continuity of heat flux at their interface, i.e.

$$K_1 \frac{\partial T_1}{\partial x} = K_2 \frac{\partial T_2}{\partial x}$$

and temperature continuity

$$T_1 = T_2$$

Here x is the coordinate on the axis which is perpendicular to the interface between the bodies and is directed from the second body to the first one; T_1 and T_2 are the temperatures of the first and second bodies, respectively; K_1 and K_2 are the thermal conductivities of the first and second bodies, respectively. The two conditions above are often referred to as 'perfect thermal contact'.

Blok [3] considered a thermal interaction of two bodies sliding in a local region with friction heat generation. The heat-partition coefficient α_f was defined to satisfy the requirement that the maximum stationary temperature in the sliding region of the first body is equal to that of the second body. This coefficient indicates the fraction of friction heat dissipated in the first body and, thereby, allows explicit specification of heat partition between the bodies:

$$-K_1 \frac{\partial T_1}{\partial x} = \alpha_\mathrm{f} q; \qquad K_2 \frac{\partial T_2}{\partial x} = (1 - \alpha_\mathrm{f}) q \tag{1}$$

The specific power q of heat generation is determined from the equality

$$q = \mu p v$$

where μ is the friction coefficient; p is the contact pressure; v is the sliding velocity. The advantage of Eq.(1) lies in the possibility to split temperature fields of the bodies and investigate them separately from each other. Various approaches to determination of α_f were examined by Jaeger [4], Charron [5], Archard [6] and others.

The partition of friction heat due to constant α_f is consistent with temperature continuity at the sliding interface only for a narrow class of geometrically one-dimensional problems (Nosko [7]). Application of Eq.(1) generally results in a temperature jump when passing from one body to the other. Ling [8] proposed alternative boundary conditions which require thermal balance and temperature continuity at each point of a local region of sliding:

$$-K_1 \frac{\partial T_1}{\partial x} + K_2 \frac{\partial T_2}{\partial x} = q; \qquad (2)$$
$$T_1 = T_2$$

The conditions of Eq.(2) along with a temperature expression for a heat source moving on the surface of a semispace (Carslaw and Jaeger [9], p.266–270) yield an integral equation with respect to the heat flux into one of the bodies (Cameron et al. [10]). Besides, they are often specified at the nominal sliding interface.

Podstrigach [11] considered a thermal contact of two bodies through a thin intermediate layer. By linearising temperature in the layer and introducing the contact heat transfer coefficient h_c, the layer was eliminated and the bodies were directly coupled with imperfect thermal contact conditions. Their particular case, however in the presence of a heat source, is written in our notation as

$$-K_1 \frac{\partial T_1}{\partial x} + K_2 \frac{\partial T_2}{\partial x} = q; \qquad (3)$$
$$K_1 \frac{\partial T_1}{\partial x} + K_2 \frac{\partial T_2}{\partial x} = 2h_\mathrm{c}(T_1 - T_2)$$

The coefficient h_c indicates the heat flux through the interface caused by a unit difference in the contact temperatures of the bodies. It’s noteworthy that Eq.(3) given at q=0 had been previously used in an analytical study by Mersman [12].

Barber [13] investigated heat-conduction problems of sliding, assuming that the heat flux passing in either of the bodies consists of two components: the first one is due to the generation of friction heat, while the second one is caused by the temperature difference of the bodies. This assumption leads to another type of imperfect thermal contact (Berry and Barber [14]), which in our notation reads

$$-K_1 \frac{\partial T_1}{\partial x} = \alpha q - h_\mathrm{c}(T_1 - T_2); \qquad (4)$$
$$K_2 \frac{\partial T_2}{\partial x} = (1-\alpha) q + h_\mathrm{c}(T_1 - T_2)$$

where α is the heat-generation coefficient determined by the thermal resistances of the sliding rough surfaces. Independently, Protasov [15] (p.51–73) investigated the heat generation from adhesion-deformational interactions of roughness asperities. The coefficient α was defined as the fraction of friction energy generated at the sliding surface of the first body. Theoretical studies of α were performed by Bardon [16], Laraqi [17], Chantrenne and Raynaud [18] and others. An early study by Shaaf [19] should be also noted in which a problem of heat conduction in sliding semispaces was analytically solved for Eq.(4).

Numerous studies have been focussed on simulating a frictional interaction between two asperities with account of spatial distribution of temperature in their sliding region and its vicinity. Heat-conduction simulation of the roughness asperities interaction is commonly performed under the conditions of Eq.(2) with the aid of numerical methods (Cameron et al. [10], Symm [20], Bos and Moes [21]). Nanoscale friction is simulated using the methods of Molecular Dynamics (Li et al. [22], Chen et al. [23]). The mentioned approaches allow determining temperature and its relationship with various physical processes at micro- and nanoscale. These results may be utilised for macroscopic temperature analysis through superimposing the temperature rises caused by the interactions in multiple sliding regions, which however requires accurate data on the geometry of the sliding regions. Of practical importance is their utilisation for determining the parameters incorporated into the conditions of Eq.(1), Eq.(3) and Eq.(4).

Sliding is often accompanied by the formation on contact surfaces of so-called friction layers, which has a drastic impact on the tribological characteristics. In particular, this phenomenon is widely observed in brake friction pairs (Eriksson and Jacobson [24], Filip et al. [25]). Thermal properties of friction layers differ substantially from those of the bulk materials. For instance, a steel-on-steel sliding results in the occurrence of layers of iron oxides FeO, Fe_2O_3 and Fe_3O_4 (So et al. [26]). Measurements by Akiyama et al. [27] showed that the thermal conductivity of iron at 300 °C is about 53 W/(m °C), whereas it is several times lower for the iron oxides: about 23, 17 and 5 W/(m °C) for Fe_3O_4, Fe_2O_3 and FeO, respectively. Loizou et al. [28] performed temperature simulations in a brake pair with a friction layer. The thermal conductivities of the pad and disc were set equal to 0.9 and 48 W/(m °C), respectively. It was assumed that the friction layer is composed by 80% of the pad material and by 20% of the disc material. Based on this proportion, the thermal conductivity of the friction layer was calculated to be 10 W/(m °C). In a study by Straffelini et al. [29], investigating temperature in a pin-on-disc system affected by friction layers, the thermal conductivities of the pin material and the friction layer on the pin surface were accepted equal to 0.9 and 0.07 W/(m °C), respectively.

One of the efficient ways to improve the performance of friction materials is utilisation of tribological coatings. These coatings allow one to control the level of friction, reduce wear rate, increase corrosion resistance, etc. (Holmberg et al. [30], Hogmark et al. [31], Donnet and Erdemir [32], Kindrachuk et al. [33]). The thermal conductivity of coating materials has a large scatter. For instance, it is as small as 2 W/(m °C) [34] (p.246) for zirconium dioxide, used as a thermal insulation material, and as large as 400 W/(m °C) [35] (p.68) for copper, used to provide electrical contact.

Literature review shows that the thicknesses of friction layers and coatings have magnitudes of different orders — from nanometres to hundreds of micrometres. In many practical cases, they are of several micrometres and larger. There is thus a class of problems of sliding where friction layers and coatings of considerable thicknesses and thermal conductivities differing substantially from those of the bulk materials may have a significant temperature influence. For brevity, the terms 'friction layer' and 'tribological coating' are referred to hereafter as 'surface layer'.

Thermal problem of sliding between two bodies covered with continuous surface layers represents a heat-conduction problem for a multilayer system, which is cumbersome and inefficient for analytical and numerical studies. In order to simplify it, one can attempt to simulate the temperature influence of the surface layers using special boundary conditions (Shevchuk [36]). One of the approaches to their derivation is based on imposing certain restrictions on the temperature distributions in the surface layers (Podstrigach and Shevchuk [37], Shevchuk [38], Nosko et al. [39]).

The purpose of the present study was by using the mentioned approach to derive the thermal boundary conditions which would enable efficient simulation of surface layers at sliding contacts and investigate these conditions in terms of accuracy, practical applicability and relation with well-known boundary conditions.

2. Thermal boundary conditions of sliding

2.1. Thermal processes in the surface layers

Consider two bodies sliding against each other, as schematically shown in Fig.1. The temperatures $T_1(x,t)$ and $T_2(x,t)$ of the bodies change with time t due to heat conduction. Each ith body consists of a bulk part, with thermal conductivity K_i and thermal diffusivity k_i, and a surface layer of thickness h_i, with thermal conductivity K_{si} and thermal diffusivity k_{si}, $i \in \{1,2\}$. The heat-conduction equations for the surface layers are given as follows:

$$\begin{aligned} &\frac{\partial T_1(x,t)}{\partial t} = k_{s1}\frac{\partial^2 T_1(x,t)}{\partial x^2}, \qquad 0 < x < h_1, \qquad t > 0; \\ &\frac{\partial T_2(x,t)}{\partial t} = k_{s2}\frac{\partial^2 T_2(x,t)}{\partial x^2}, \qquad -h_2 < x < 0, \qquad t > 0 \end{aligned} \tag{5}$$

The friction heat is generated with specific power $q(t)$. Its fraction α is generated at the sliding surface of the first body and, accordingly, $(1-\alpha)$ at the sliding surface of the second body. There is a heat transfer between the surface layers at the sliding interface specified by the roughness contact heat transfer coefficient γ. Thereby, the conditions at the sliding interface take the form

$$\begin{aligned} &-K_{s1}\frac{\partial T_1}{\partial x}\bigg|_{x=0+0} = \alpha q - \gamma\left(T_1|_{x=0+0} - T_2|_{x=0-0}\right); \\ &K_{s2}\frac{\partial T_2}{\partial x}\bigg|_{x=0-0} = (1-\alpha)q + \gamma\left(T_1|_{x=0+0} - T_2|_{x=0-0}\right) \end{aligned} \tag{6}$$

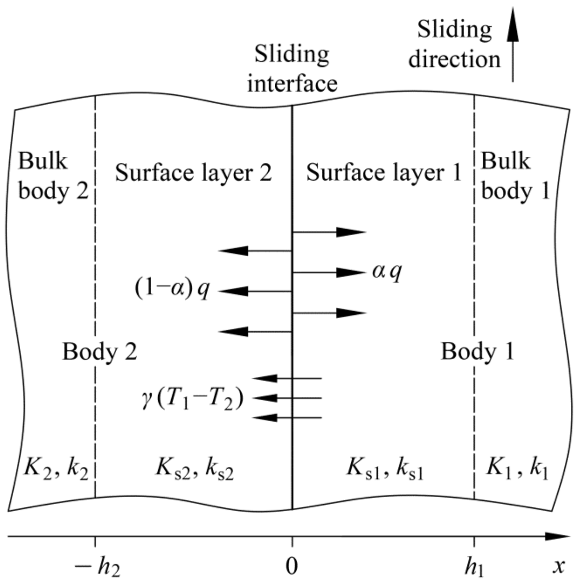

Fig.1. Schematic of the thermal processes in the surface layers (1-column image)

In fact, Eq.(6) represents the imperfect thermal contact conditions given by Eq.(4) with the only difference that the coefficient γ is used instead of h_c. The contact heat transfer coefficient h_c (also referred to as 'thermal contact conductance') is generally defined to characterise the interfacial heat transfer between bodies caused by various factors including the interaction of roughness asperities and the presence of surface layers (Lienhard IV and Lienhard V [40], p.65), whereas the introduced coefficient γ is associated only with the interaction of roughness asperities. The introduction of γ allows thus to avoid ambiguous interpretation of h_c.

Temperature continuity is specified at the boundaries between the corresponding bulk bodies and surface layers:

$$
\begin{aligned}
&K_1 \left.\frac{\partial T_1}{\partial x}\right|_{x=h_1+0} = K_{s1} \left.\frac{\partial T_1}{\partial x}\right|_{x=h_1-0}; \\
&T_1|_{x=h_1+0} = T_1|_{x=h_1-0}; \\
&K_2 \left.\frac{\partial T_2}{\partial x}\right|_{x=-h_2-0} = K_{s2} \left.\frac{\partial T_2}{\partial x}\right|_{x=-h_2+0}; \\
&T_2|_{x=-h_2-0} = T_2|_{x=-h_2+0}
\end{aligned}
\tag{7}
$$

2.2. Derivation of the boundary conditions

Assume linear temperature distributions in the surface layers. Consequently, it is true that

$$
\begin{aligned}
&T_1|_{x=0+0} = \left.\left(T_1 - h_1 \frac{\partial T_1}{\partial x}\right)\right|_{x=h_1-0}; \\
&T_2|_{x=0-0} = \left.\left(T_2 + h_2 \frac{\partial T_2}{\partial x}\right)\right|_{x=-h_2+0}
\end{aligned}
\tag{8}
$$

The average temperatures of the surface layers are then determined as follows:

$$\frac{1}{h_1}\int_0^{h_1} T_1 dx = \frac{T_1|_{x=0+0} + T_1|_{x=h_1-0}}{2} = \left(T_1 - \frac{h_1}{2}\frac{\partial T_1}{\partial x}\right)\bigg|_{x=h_1-0};$$
$$\frac{1}{h_2}\int_{-h_2}^{0} T_2 dx = \frac{T_2|_{x=-h_2+0} + T_2|_{x=0-0}}{2} = \left(T_2 + \frac{h_2}{2}\frac{\partial T_2}{\partial x}\right)\bigg|_{x=-h_2+0} \quad (9)$$

Integrate Eq.(5) over the corresponding domains of the surface layers. Based on Eq.(7) and Eq.(9), integration of the left sides yields

$$\frac{1}{h_1}\int_0^{h_1} \frac{\partial T_1}{\partial t} dx = \frac{\partial}{\partial t}\left(\frac{1}{h_1}\int_0^{h_1} T_1 dx\right) = \left(\frac{\partial T_1}{\partial t} - \frac{K_1 h_1}{2K_{s1}}\frac{\partial^2 T_1}{\partial t \partial x}\right)\bigg|_{x=h_1+0};$$
$$\frac{1}{h_2}\int_{-h_2}^{0} \frac{\partial T_2}{\partial t} dx = \frac{\partial}{\partial t}\left(\frac{1}{h_2}\int_{-h_2}^{0} T_2 dx\right) = \left(\frac{\partial T_2}{\partial t} + \frac{K_2 h_2}{2K_{s2}}\frac{\partial^2 T_2}{\partial t \partial x}\right)\bigg|_{x=-h_2-0} \quad (10)$$

The right sides of Eq.(5) are transformed with account of Eq.(6), Eq.(7) and Eq.(8) as follows:

$$\frac{1}{h_1}\int_0^{h_1} k_{s1}\frac{\partial^2 T_1}{\partial x^2} dx = \frac{k_{s1}}{h_1}\frac{\partial T_1}{\partial x}\bigg|_{x=h_1-0} - \frac{k_{s1}}{h_1}\frac{\partial T_1}{\partial x}\bigg|_{x=0+0}$$
$$= \frac{\alpha q k_{s1}}{K_{s1}h_1} - \frac{k_{s1}}{K_{s1}h_1}\left(\gamma T_1 - K_1\left(1 + \frac{\gamma h_1}{K_{s1}}\right)\frac{\partial T_1}{\partial x}\right)\bigg|_{x=h_1+0} + \frac{\gamma k_{s1}}{K_{s1}h_1}\left(T_2 + \frac{K_2 h_2}{K_{s2}}\frac{\partial T_2}{\partial x}\right)\bigg|_{x=-h_2-0};$$
$$\frac{1}{h_2}\int_{-h_2}^{0} k_{s2}\frac{\partial^2 T_2}{\partial x^2} dx = \frac{k_{s2}}{h_2}\frac{\partial T_2}{\partial x}\bigg|_{x=0-0} - \frac{k_{s2}}{h_2}\frac{\partial T_2}{\partial x}\bigg|_{x=-h_2+0} = \frac{(1-\alpha)q k_{s2}}{K_{s2}h_2}$$
$$+ \frac{\gamma k_{s2}}{K_{s2}h_2}\left(T_1 - \frac{K_1 h_1}{K_{s1}}\frac{\partial T_1}{\partial x}\right)\bigg|_{x=h_1+0} - \frac{k_{s2}}{K_{s2}h_2}\left(\gamma T_2 + K_2\left(1 + \frac{\gamma h_2}{K_{s2}}\right)\frac{\partial T_2}{\partial x}\right)\bigg|_{x=-h_2-0} \quad (11)$$

Equating the corresponding expressions of Eq.(10) and Eq.(11) and introducing the thermal resistance $r_i = h_i/K_{si}$ and heat capacity $c_i = K_{si}h_i/k_{si}$ (per unit friction area) of each ith surface layer give

$$\left(\gamma T_1 + c_1\frac{\partial T_1}{\partial t} - K_1(1+\gamma r_1)\frac{\partial T_1}{\partial x} - \frac{c_1 K_1 r_1}{2}\frac{\partial^2 T_1}{\partial t \partial x}\right)\bigg|_{x=h_1+0} - \gamma\left(T_2 + K_2 r_2\frac{\partial T_2}{\partial x}\right)\bigg|_{x=-h_2-0}$$
$$= \alpha q;$$
$$-\gamma\left(T_1 - K_1 r_1\frac{\partial T_1}{\partial x}\right)\bigg|_{x=h_1+0} + \left(\gamma T_2 + c_2\frac{\partial T_2}{\partial t} + K_2(1+\gamma r_2)\frac{\partial T_2}{\partial x} + \frac{c_2 K_2 r_2}{2}\frac{\partial^2 T_2}{\partial t \partial x}\right)\bigg|_{x=-h_2-0}$$
$$= (1-\alpha)q \quad (12)$$

Note that the temperatures $T_i(x,t)$ and their derivatives in Eq.(12) are taken at $x = h_1 + 0$ or $x = -h_2 - 0$, i.e. these quantities are related to the bulk bodies.

By eliminating the surface layers from consideration and merging the bulk bodies, the following boundary conditions are finally obtained from Eq.(12):

$$-K_1\frac{\partial T_1}{\partial x}=\alpha q-\gamma\left(T_1-T_2-K_1r_1\frac{\partial T_1}{\partial x}-K_2r_2\frac{\partial T_2}{\partial x}\right)-c_1\frac{\partial}{\partial t}\left(T_1-\frac{K_1r_1}{2}\frac{\partial T_1}{\partial x}\right);$$
$$K_2\frac{\partial T_2}{\partial x}=(1-\alpha)q+\gamma\left(T_1-T_2-K_1r_1\frac{\partial T_1}{\partial x}-K_2r_2\frac{\partial T_2}{\partial x}\right)-c_2\frac{\partial}{\partial t}\left(T_2+\frac{K_2r_2}{2}\frac{\partial T_2}{\partial x}\right) \tag{13}$$

The conditions of Eq.(13) are thus formulated for the bulk bodies but with allowance for the presence of the surface layers (parameters r_i and c_i) and the interaction of roughness asperities (parameters α and γ).

2.3. Relation with well-known boundary conditions

Figure 2 presents important particular cases of Eq.(13). If the thermal resistances r_i are negligibly small, which can be caused by large values of K_{si}, Eq.(13) transforms into

$$-K_1\frac{\partial T_1}{\partial x}=\alpha q-\gamma(T_1-T_2)-c_1\frac{\partial T_1}{\partial t};$$
$$K_2\frac{\partial T_2}{\partial x}=(1-\alpha)q+\gamma(T_1-T_2)-c_2\frac{\partial T_2}{\partial t} \tag{14}$$

On the other hand, neglecting the heat capacities c_i of the surface layers in Eq.(13) results in

$$-K_1\frac{\partial T_1}{\partial x}=\alpha q-\gamma\left(T_1-T_2-K_1r_1\frac{\partial T_1}{\partial x}-K_2r_2\frac{\partial T_2}{\partial x}\right);$$
$$K_2\frac{\partial T_2}{\partial x}=(1-\alpha)q+\gamma\left(T_1-T_2-K_1r_1\frac{\partial T_1}{\partial x}-K_2r_2\frac{\partial T_2}{\partial x}\right) \tag{15}$$

The case above can happen at small ratios $K_{\mathrm{s}i}/k_{\mathrm{s}i}$ which represent the volumetric heat capacities of the materials of the surface layers

Of interest are also the particular cases related to the heat transfer at the sliding interface. For infinitely intensive contact heat transfer, i.e. $\gamma\to\infty$, Eq.(13) degenerates into

$$-K_1\frac{\partial T_1}{\partial x}+K_2\frac{\partial T_2}{\partial x}=q-c_1\frac{\partial}{\partial t}\left(T_1-\frac{K_1r_1}{2}\frac{\partial T_1}{\partial x}\right)-c_2\frac{\partial}{\partial t}\left(T_2+\frac{K_2r_2}{2}\frac{\partial T_2}{\partial x}\right);$$
$$K_1r_1\frac{\partial T_1}{\partial x}+K_2r_2\frac{\partial T_2}{\partial x}=T_1-T_2 \tag{16}$$

Note that Eq.(16) implies the equality of the temperatures of the surface layers at the sliding interface (but $T_1\neq T_2$ for the bulk bodies).

On the contrary, if there is no contact heat transfer, i.e. γ=0, it yields from Eq.(13) that

$$-K_1\frac{\partial T_1}{\partial x}=\alpha q-c_1\frac{\partial}{\partial t}\left(T_1-\frac{K_1r_1}{2}\frac{\partial T_1}{\partial x}\right);$$
$$K_2\frac{\partial T_2}{\partial x}=(1-\alpha)q-c_2\frac{\partial}{\partial t}\left(T_2+\frac{K_2r_2}{2}\frac{\partial T_2}{\partial x}\right) \tag{17}$$

Depending on the parameters, each of Eq.(14), Eq.(15) and Eq.(16) can transform into the imperfect thermal contact conditions of Eq.(4), while Eq.(17) turns into the heat-partition conditions of Eq.(1) when c_i=0, as shown in Fig.2.

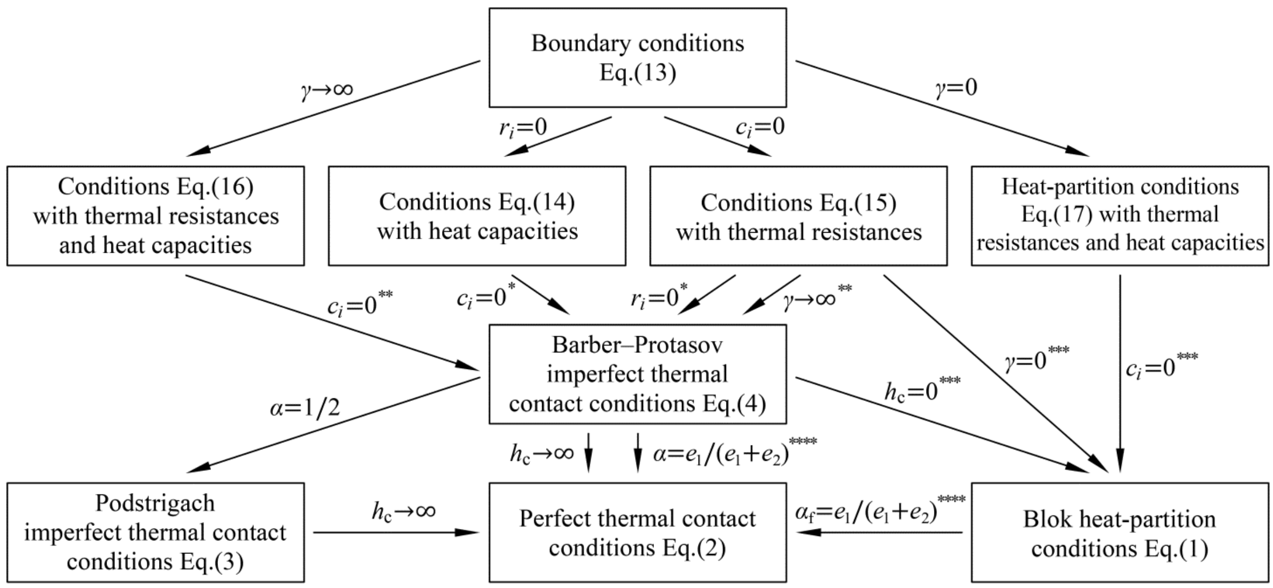

Fig.2. Classification of the thermal boundary conditions of sliding (2-column image)

* $h_c = \gamma$; ** $\alpha = r_2/(r_1+r_2)$ and $h_c = 1/(r_1+r_2)$ [14];

*** $\alpha_f = \alpha$; **** valid for the contact of semispaces [9] (p.88)

There are two qualitatively different transformation chains from Eq.(13) to Eq.(4). One of them corresponds to the absence of the surface layers, i.e. $r_i = c_i = 0$. The coefficient h_c in this case coincides with γ. The other transformation chain implies c_i=0 and $\gamma \to \infty$, and the coefficients α and h_c are solely determined by r_1 and r_2. Furthermore, Eq.(4) can in its turn transform into Eq.(1), Eq.(2) or Eq.(3).

3. Sliding between semispaces covered with surface layers

Consider two semispaces covered with surface layers that are in sliding motion. Heat conduction in the semispaces is described by the equations

$$\begin{aligned} &\frac{\partial T_1(x,t)}{\partial t} = k_1 \frac{\partial^2 T_1(x,t)}{\partial x^2}, \qquad x>0, \qquad t>0; \\ &\frac{\partial T_2(x,t)}{\partial t} = k_2 \frac{\partial^2 T_2(x,t)}{\partial x^2}, \qquad x<0, \qquad t>0 \end{aligned} \tag{18}$$

The thermal processes at the sliding interface and in the surface layers are simulated using the derived conditions of Eq.(13) assigned to the point x=0. Temperature gradient at infinite distance from the sliding interface is zero, i.e.

$$\left.\frac{\partial T_1}{\partial x}\right|_{x\to+\infty} = \left.\frac{\partial T_2}{\partial x}\right|_{x\to-\infty} = 0 \tag{19}$$

At the initial instance of time t=0, the semispaces have zero temperature distributions:

$$T_1|_{t=0} = T_2|_{t=0} = 0 \tag{20}$$

An analytical solution of Eqs.(13),(18)–(20) can be obtained by applying the Laplace transform approach.

3.1. Solution in images of the Laplace transform

Assume that the functions $T_i(x,t)$ and $q(t)$ are originals of the Laplace transform $\mathcal{L}$ with respect to the time variable t, i.e. there exist images $\tilde{T}_i(x,s) = \mathcal{L}[T_i(x,t)]$ and $\tilde{q}(s) = \mathcal{L}[q(t)]$. Here s is the transform parameter. It is easy to verify that the following sets of functions satisfy Eq.(18), Eq.(19) and Eq.(20) in the space of images:

$$\begin{aligned} \tilde{T}_1(x,s) &= A_1(s)\exp\left\{-x\sqrt{s/k_1}\right\}; \\ \tilde{T}_2(x,s) &= A_2(s)\exp\left\{x\sqrt{s/k_2}\right\} \end{aligned} \tag{21}$$

By substituting Eq.(21) into Eq.(13) in the space of images and setting x=0, a system of equations is derived with respect to $A_1(s)$ and $A_2(s)$ as follows:

$$\begin{aligned} &\left(\gamma + e_1(1+\gamma r_1)\sqrt{s} + c_1 s + \frac{c_1 e_1 r_1}{2} s\sqrt{s}\right) A_1(s) - \gamma\left(1 + e_2 r_2\sqrt{s}\right)A_2(s) = \alpha\tilde{q}(s); \\ &-\gamma\left(1 + e_1 r_1\sqrt{s}\right)A_1(s) + \left(\gamma + e_2(1+\gamma r_2)\sqrt{s} + c_2 s + \frac{c_2 e_2 r_2}{2} s\sqrt{s}\right) A_2(s) = (1-\alpha)\tilde{q}(s) \end{aligned} \tag{22}$$

where $e_i = K_i/\sqrt{k_i}$ is the thermal effusivity of the ith semispace. The solution of Eq.(22) allows expressing Eq.(21) as

$$\begin{aligned} \tilde{T}_1(x,s) &= \tilde{q}(s)\,\tilde{\varphi}_1(x,s); \\ \tilde{T}_2(x,s) &= \tilde{q}(s)\,\tilde{\varphi}_2(x,s) \end{aligned} \tag{23}$$

where

$$\begin{aligned} \tilde{\varphi}_1(x,s) &= \frac{\left(b_{10} + b_{11}\sqrt{s} + b_{12}s + b_{13}s\sqrt{s}\right)\exp\left\{-x\sqrt{s/k_1}\right\}}{\sqrt{s}\left(a_0 + a_1\sqrt{s} + a_2 s + a_3 s\sqrt{s} + a_4 s^2 + a_5 s^2\sqrt{s}\right)}; \\ \tilde{\varphi}_2(x,s) &= \frac{\left(b_{20} + b_{21}\sqrt{s} + b_{22}s + b_{23}s\sqrt{s}\right)\exp\left\{x\sqrt{s/k_2}\right\}}{\sqrt{s}\left(a_0 + a_1\sqrt{s} + a_2 s + a_3 s\sqrt{s} + a_4 s^2 + a_5 s^2\sqrt{s}\right)} \end{aligned} \tag{24}$$

with the coefficients

$$\begin{aligned} a_0 &= \gamma(e_1 + e_2); \\ a_1 &= e_1 e_2 + \gamma\left(c_1 + c_2 + e_1 e_2(r_1 + r_2)\right); \\ a_2 &= c_1 e_2 + c_2 e_1 + \gamma\left(e_1 r_1(c_1/2 + c_2) + e_2 r_2(c_1 + c_2/2)\right); \\ a_3 &= c_1 c_2 + e_1 e_2\left(c_1 r_1 + c_2 r_2 + \gamma r_1 r_2(c_1 + c_2)\right)/2\,; \\ a_4 &= c_1 c_2(e_1 r_1 + e_2 r_2)/2\,; \\ a_5 &= c_1 c_2 e_1 e_2 r_1 r_2/4; \\ b_{10} &= \gamma; \end{aligned}$$

$$b_{11} = e_2(\alpha + \gamma r_2);$$
$$b_{12} = \alpha c_2;$$
$$b_{13} = \alpha c_2 e_2 r_2/2\,;$$
$$b_{20} = \gamma;$$
$$b_{21} = e_1(1 - \alpha + \gamma r_1);$$
$$b_{22} = (1 - \alpha)c_1;$$
$$b_{23} = (1 - \alpha)c_1 e_1 r_1/2$$

Note that the coefficients above take only non-negative values.

3.2. Solution in the time domain

Restore the originals of Eq.(23) and represent them in the form of convolutions:

$$T_i(x,t) = \int_0^t q(t-\tau)\varphi_i(x,\tau)\,d\tau \tag{25}$$

where $\varphi_i(x,t) = \mathcal{L}^{-1}[\tilde{\varphi}_i(x,s)]$.

The originals $\varphi_i(x,t)$ can be found by calculating the Mellin integral in the inverse Laplace transform (Carslaw and Jaeger [9], p.302–304). Fig. 3 presents the integration contour Γ in the complex plane s. Γ consists of a line segment AB parallel to the imaginary axis Im s, circle arcs BC and FA of radius R centred at the origin O, line segments CD and EF parallel to the real axis Re s, and a circle arc DE of radius ρ centred at O. The functions $\tilde{\varphi}_i(x,s)$ of Eq.(24) have a singularity at s=0 which is the branch point of the double-valued function $\sqrt{s}$. Choose its branch $g_0(s)$ which satisfies the equality $g_0(1) = 1$. Then the functions $\tilde{\varphi}_i(x,s)$ are single-valued analytical within Γ and continuous both within Γ and along its boundary. According to the Cauchy integral theorem, when $R \to \infty$ and $\rho \to 0$ the integral along AB is equal to the sum of the integrals along BC, CD, DE, EF and FA:

$$\begin{aligned}\varphi_i(x,t) = -\frac{1}{2\pi j}\lim_{\substack{R\to\infty\\ \rho\to 0}}\Bigg(&\int_{\mathrm{BC}\cup\mathrm{FA}} \tilde{\varphi}_i(x,s)\exp\{st\}\,ds + \int_{\mathrm{CD}} \tilde{\varphi}_i(x,s)\exp\{st\}\,ds \\ &+ \int_{\mathrm{DE}} \tilde{\varphi}_i(x,s)\exp\{st\}\,ds + \int_{\mathrm{EF}} \tilde{\varphi}_i(x,s)\exp\{st\}\,ds\Bigg)\end{aligned} \tag{26}$$

where j is the imaginary unit.

The functions $\tilde{\varphi}_i(x,s)$ satisfy the conditions of the Jordan lemma. Consequently, when $R \to \infty$ the integral along the arcs BC and FA tends to zero:

$$\lim_{R\to\infty}\int_{\mathrm{BC}\cup\mathrm{FA}} \tilde{\varphi}_i(x,s)\exp\{st\}\,ds = 0 \tag{27}$$

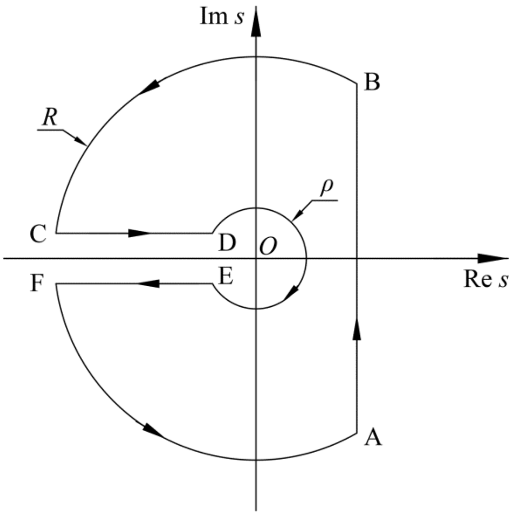

Fig.3. Integration contour Γ in the complex plane s (1-column image)

For the arc DE, it is true that $s = \rho \exp\{j \arg(s)\}$. When $\rho \to 0$ the integral along this arc tends to zero as well:

$$\lim_{\rho \to 0} \int_{\mathrm{DE}} \tilde{\varphi}_i(x, s) \exp\{st\}\, ds = 0 \tag{28}$$

Furthermore, accepting $s = z^2 \exp\{j\pi\} = -z^2$ and $\sqrt{s} = z \exp\{j\pi/2\} = jz$ for $s \in$ CD, while $s = z^2 \exp\{-j\pi\} = -z^2$ and $\sqrt{s} = z \exp\{-j\pi/2\} = -jz$ for $s \in$ EF, one can express the corresponding integrals as

$$\lim_{\substack{R \to \infty \\ \rho \to 0}} \int_{\mathrm{CD}} \tilde{\varphi}_1(x, s) \exp\{st\}\, ds$$
$$= 2 \int_0^\infty \frac{\left(b_{10} - b_{12} z^2 + j(b_{11} z - b_{13} z^3)\right) \exp\left\{-jxz/\sqrt{k_1}\right\}}{-a_1 z + a_3 z^3 - a_5 z^5 + j(a_0 - a_2 z^2 + a_4 z^4)} \exp\{-z^2 t\}\, dz\,;$$

(29)

$$\lim_{\substack{R \to \infty \\ \rho \to 0}} \int_{\mathrm{CD}} \tilde{\varphi}_2(x, s) \exp\{st\}\, ds$$
$$= 2 \int_0^\infty \frac{\left(b_{20} - b_{22} z^2 + j(b_{21} z - b_{23} z^3)\right) \exp\left\{jxz/\sqrt{k_2}\right\}}{-a_1 z + a_3 z^3 - a_5 z^5 + j(a_0 - a_2 z^2 + a_4 z^4)} \exp\{-z^2 t\}\, dz$$

and

$$\lim_{\substack{R\to\infty\\ \rho\to 0}} \int_{\mathrm{EF}} \tilde{\varphi}_1(x,s)\exp\{st\}\,ds$$
$$= -2\int_0^\infty \frac{\left(b_{10} - b_{12}z^2 - j(b_{11}z - b_{13}z^3)\right)\exp\{jxz/\sqrt{k_1}\}}{-a_1z + a_3z^3 - a_5z^5 - j(a_0 - a_2z^2 + a_4z^4)}\exp\{-z^2t\}\,dz\,;$$
$$\lim_{\substack{R\to\infty\\ \rho\to 0}} \int_{\mathrm{EF}} \tilde{\varphi}_2(x,s)\exp\{st\}\,ds$$
$$= -2\int_0^\infty \frac{\left(b_{20} - b_{22}z^2 - j(b_{21}z - b_{23}z^3)\right)\exp\{-jxz/\sqrt{k_2}\}}{-a_1z + a_3z^3 - a_5z^5 - j(a_0 - a_2z^2 + a_4z^4)}\exp\{-z^2t\}\,dz \tag{30}$$

Finally, substitution of Eqs.(27)–(30) into Eq.(26) and introduction of the functions

$$D(z) = (-a_1z + a_3z^3 - a_5z^5)^2 + (a_0 - a_2z^2 + a_4z^4)^2;$$
$$M_1(z) = (b_{10} - b_{12}z^2)(a_0 - a_2z^2 + a_4z^4) - (b_{11}z - b_{13}z^3)(-a_1z + a_3z^3 - a_5z^5);$$
$$N_1(z) = (b_{10} - b_{12}z^2)(-a_1z + a_3z^3 - a_5z^5) + (b_{11}z - b_{13}z^3)(a_0 - a_2z^2 + a_4z^4);$$
$$M_2(z) = (b_{20} - b_{22}z^2)(a_0 - a_2z^2 + a_4z^4) - (b_{21}z - b_{23}z^3)(-a_1z + a_3z^3 - a_5z^5);$$
$$N_2(z) = (b_{20} - b_{22}z^2)(-a_1z + a_3z^3 - a_5z^5) + (b_{21}z - b_{23}z^3)(a_0 - a_2z^2 + a_4z^4)$$

give

$$\varphi_1(x,t) = \frac{2}{\pi}\int_0^\infty \left(\frac{M_1(z)}{D(z)}\cos\left(\frac{xz}{\sqrt{k_1}}\right) + \frac{N_1(z)}{D(z)}\sin\left(\frac{xz}{\sqrt{k_1}}\right)\right)\exp\{-z^2t\}\,dz\,;$$
$$\varphi_2(x,t) = \frac{2}{\pi}\int_0^\infty \left(\frac{M_2(z)}{D(z)}\cos\left(\frac{xz}{\sqrt{k_2}}\right) - \frac{N_2(z)}{D(z)}\sin\left(\frac{xz}{\sqrt{k_2}}\right)\right)\exp\{-z^2t\}\,dz$$

whence, with account of Eq.(25), the sought temperatures are found in the form

$$T_1(x,t) = \frac{2}{\pi}\int_0^\infty \left(\frac{M_1(z)}{D(z)}\cos\left(\frac{xz}{\sqrt{k_1}}\right) + \frac{N_1(z)}{D(z)}\sin\left(\frac{xz}{\sqrt{k_1}}\right)\right)\int_0^t q(t-\tau)\exp\{-z^2\tau\}\,d\tau\,dz\,;$$
$$T_2(x,t) = \frac{2}{\pi}\int_0^\infty \left(\frac{M_2(z)}{D(z)}\cos\left(\frac{xz}{\sqrt{k_2}}\right) - \frac{N_2(z)}{D(z)}\sin\left(\frac{xz}{\sqrt{k_2}}\right)\right)\int_0^t q(t-\tau)\exp\{-z^2\tau\}\,d\tau\,dz \tag{31}$$

If $q(t)$ is prescribed as a polynomial function, computation of Eq.(31) can be essentially simplified using the equality

$$\int_0^t (t-\tau)^m \exp\{-z^2\tau\}\,d\tau = \frac{m!}{(-z^2)^{1+m}}\left(\exp\{-z^2t\} - \sum_{n=0}^{m}\frac{(-z^2t)^n}{n!}\right)$$

where m is a non-negative integer.

3.3. Comparison with known temperature expressions

Analysis shows that the particular cases of Eq.(31) match the exact temperature expressions derived by Carslaw and Jaeger [9], Shaaf [19], Grilitskii [41], Krasnyuk [42], Matysiak et al. [43, 44], Pyr'ev [45], de Monte [46], Yevtushenko and Kuciej [47–50], Belyakov and Nosko [51–53], Dülk and Kovácsházy [54].

For example, consider a decelerative sliding between a low-metallic brake material (T_1), with K_1=2 W/(m °C) and k_1=0.3·10^{-6} m^2/s, and a cast iron (T_2), with K_2=60 W/(m °C) and k_2=12·10^{-6} m^2/s. The contact heat transfer occurs with h_c=500 W/(m^2 °C). The heat-generation specific power decreases linearly from the initial value q_0=1.4·10^6 W/m^2 to zero during t_0=5 s:

$$q(t) = q_0 \left(1 - \frac{t}{t_0}\right) \tag{32}$$

Fig.4 illustrates the simulation results. The temperatures of Eq.(31) calculated at $r_i = c_i = 0, \gamma = h_c$ and x=0 agree with the solution by Carslaw and Jaeger [9] (p.88) for Eq.(2) at $\alpha = e_1/(e_1 + e_2) \approx 0.17$, solution by Shaaf [19] for Eq.(4) at α=0.35, and solution by Yevtushenko and Kuciej [50] for Eq.(3) at α=1/2. The relationship between the considered boundary conditions was previously presented in Fig.2.

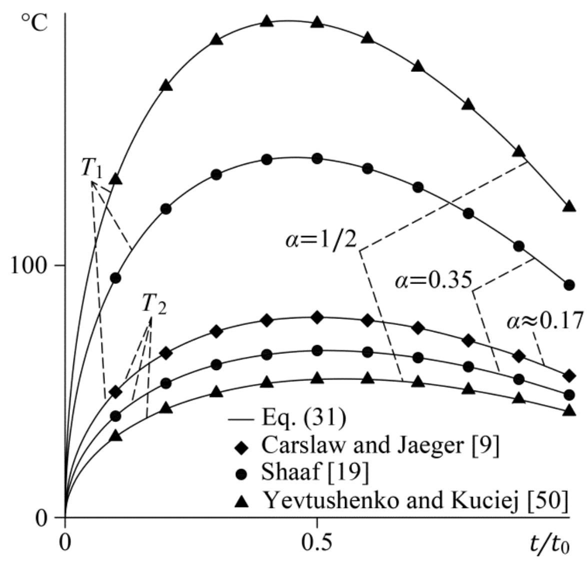

Fig.4. Comparison of Eq.(31) with known temperature expressions (1-column image)

4. Sliding between a semispace covered with a surface layer and a constant-temperature semispace

There are practical situations when the thermal processes in a sliding component are insignificantly affected by temperature changes in the counter-component. Investigate such a situation on example of a semispace covered with a surface layer sliding against a counter-semispace. The temperature $T(x,t)$ in the semispace is governed by its thermal conductivity K and thermal diffusivity k. The surface layer is characterised by its thickness h, thermal conductivity K_s and thermal diffusivity k_s. The temperature of the counter-semispace is constant and equals zero for definiteness. The friction heat is generated at the sliding surface of the surface layer with specific power $q(t)$. There is a heat transfer from the surface layer to the counter-semispace specified by the coefficient γ. The initial temperature of the semispace is zero. Using the boundary conditions of Eq.(13) assigned to the point x=0 allows formulating the mentioned problem as follows:

$$\begin{aligned}
&\frac{\partial T(x,t)}{\partial t} = k\frac{\partial^2 T(x,t)}{\partial x^2}, \qquad x>0, \qquad t>0;\\
&-K\frac{\partial T}{\partial x}\bigg|_{x=0} = q-\gamma\left(T-Kr\frac{\partial T}{\partial x}\right)\bigg|_{x=0} - c\frac{\partial}{\partial t}\left(T-\frac{Kr}{2}\frac{\partial T}{\partial x}\right)\bigg|_{x=0};\\
&\frac{\partial T}{\partial x}\bigg|_{x\to+\infty} = 0;\\
&T|_{t=0} = 0
\end{aligned} \tag{33}$$

where $r = h/K_\mathrm{s}$ and $c = K_\mathrm{s}h/k_\mathrm{s}$ are the thermal resistance and heat capacity (per unit friction area) of the surface layer, respectively.

The solution of Eq.(33) can be obtained by using the procedure described in the sections **3.1** and **3.2** or by setting $c_2 \to \infty$ in the temperature expression $T_1(x,t)$ of Eq.(31):

$$T(x,t) = \frac{2}{\pi} \int_0^\infty \left(\frac{\frac{zK}{\sqrt{k}}\left(1+\gamma r-\frac{cr}{2}z^2\right)\cos\left(\frac{xz}{\sqrt{k}}\right)+(\gamma-cz^2)\sin\left(\frac{xz}{\sqrt{k}}\right)}{\left(\frac{zK}{\sqrt{k}}\right)^2\left(1+\gamma r-\frac{cr}{2}z^2\right)^2+(\gamma-cz^2)^2} \right) \int_0^t q(t-\tau)\exp\{-z^2\tau\}\,d\tau\, z\, dz \tag{34}$$

Introduce the dimensionless spatial coordinate $\xi = x/h$, time variable $\mathrm{Fo} = kt/h^2$ (Fourier number), sliding duration $\mathrm{Fo}_0 = kt_0/h^2$, temperature $\vartheta = KT/(q_0 h)$, heat-generation power $Q = q/q_0$, contact heat transfer coefficient $B = \gamma h/K$, thermal conductivity ratio $\Lambda = K_\mathrm{s}/K$ and thermal diffusivity ratio $\chi = k_\mathrm{s}/k$. Here $q_0 \neq 0$ plays the role of a scale parameter. The temperature of Eq.(34) is then expressed as

$$\vartheta(\xi,\mathrm{Fo}) = \frac{2}{\pi} \int_0^\infty \frac{z\left(1+\frac{B}{\Lambda}-\frac{z^2}{2\chi}\right)\cos(\xi z)+\left(B-\frac{\Lambda}{\chi}z^2\right)\sin(\xi z)}{z^2\left(1+\frac{B}{\Lambda}-\frac{z^2}{2\chi}\right)^2+\left(B-\frac{\Lambda}{\chi}z^2\right)^2} \int_0^{\mathrm{Fo}} Q(\mathrm{Fo}-\tau)\exp\{-z^2\tau\}\,d\tau\, z\, dz \tag{35}$$

The thermal diffusivity (k) is related to the thermal conductivity (K) by the equality $k = K/c_v$, where c_v is the volumetric heat capacity. For temperatures above 0 °C, the vast majority of solid materials have c_v lying in the range of 1 to 5 J/(cm^3 °C) [55, 56], whereas K may differ by 3 orders of magnitude [34, 35]. The value of k is thus governed mainly by the value of K. This allows accepting in the following calculations that $k_\mathrm{s}/k = K_\mathrm{s}/K$ and, accordingly, $\chi = \Lambda$.

Table 1 presents the parameter variation ranges typical for friction materials and operation conditions of brakes.

Table 1. Parameter variation ranges

Parameter	Minimum order of magnitude	Maximum order of magnitude
Surface layer thickness h, m [30, 31]	10^{-8}	10^{-4}
Thermal conductivity K, W/(m °C) [34, 35]	10^{-1}	10^{2}
Thermal diffusivity k, m^2/s	10^{-7}	10^{-4}
Sliding duration t_0, s	10^{0}	10^{2}
Roughness contact heat transfer coefficient γ, W/(m^2 °C) [40] (p.66)	10^{2}	10^{4}
Thermal conductivity ratio Λ	$\mathbf{10^{-2}}$	$\mathbf{10^{2}}$
Dimensionless sliding duration $\mathbf{Fo_0}$	$\mathbf{10^{1}}$	$\mathbf{10^{14}}$
Dimensionless contact heat transfer coefficient *B*	$\mathbf{10^{-8}}$	$\mathbf{10^{1}}$

The temperature ϑ given by Eq.(35) is analysed for the decelerative sliding of Eq.(32), with special focus on its maximum value

$$\vartheta_{\max} = \max\{\vartheta\}|_{\xi=0,\ \ 0<\mathrm{Fo}\leq\mathrm{Fo}_0}$$

The values of the parameters Λ, Fo_0 and B are set according to Table 1.

Figure 5 shows the influence of Λ. At small values of Λ the surface layer acts as a thermal insulator, which results in comparatively small ϑ. An increase in Λ, implying a larger surface layer thermal conductivity (K_s), leads to an increase in $\vartheta_{\max}$.

Figure 6 illustrates the influence of Fo_0. It is shown that $\vartheta_{\max}$ increases with Fo_0. In addition, the temperature peak shifts in the direction of smaller $\mathrm{Fo}/\mathrm{Fo}_0$. These trends are explained by that for a longer sliding duration (t_0) the behaviour of ϑ depends less on the heating prehistory or, in other words, it is closer to quasi-stationary. At large values of Fo_0, the curve of ϑ lies close to that of the dimensionless heat-generation power (Q) defined by Eq.(32) and denoted by '$\mathrm{Fo}_0 \to \infty$'.

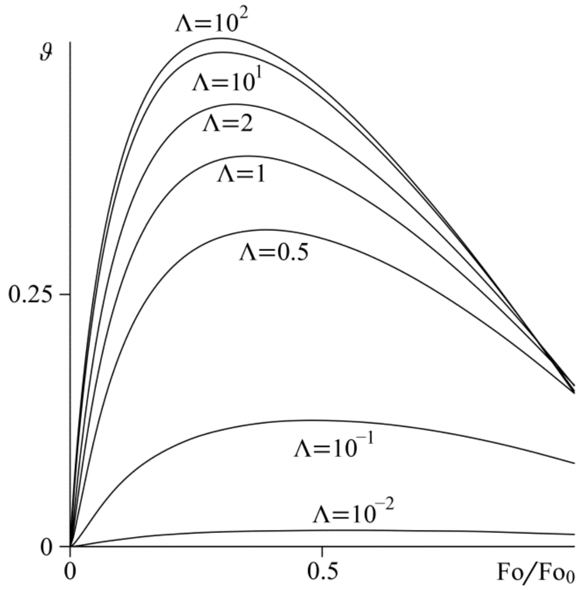

Fig.5. Influence of the thermal conductivity ratio Λ on the temperature ϑ at ξ=0, B=1 and Fo_0=10

(1-column image)

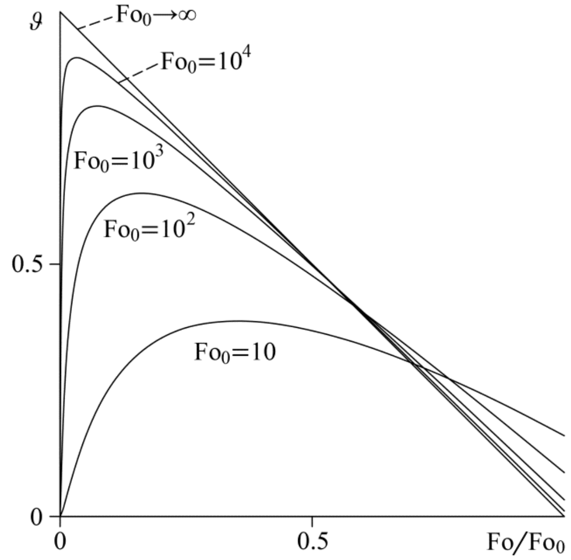

Fig.6. Influence of the sliding duration Fo_0 on the temperature ϑ at ξ=0 and $\Lambda = B = 1$ (1-column image)

Figure 7 presents the influence of B. The curve 'B=0' stands for the absence of the contact heat transfer from the surface layer to the counter-semispace. Changes in B in the range from 0 to the order of 10^{-2} have insignificant influence on ϑ. With further increase in B, the contact heat transfer becomes more intensive, which results in smaller ϑ. These results qualitatively agree with those obtained by Yevtushenko and Kuciej [48].

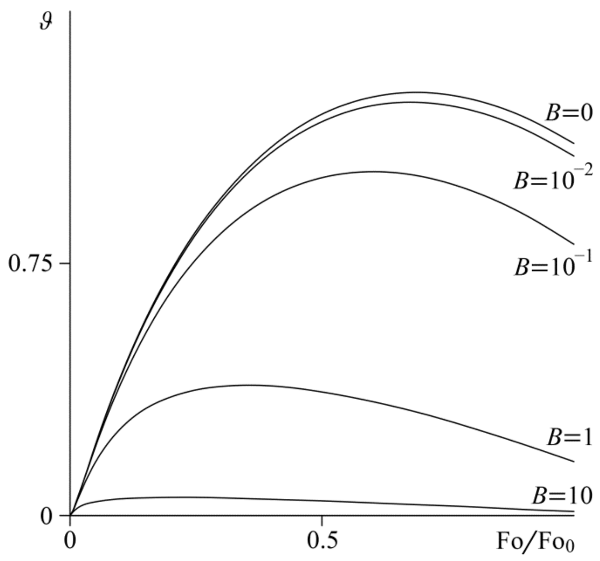

Fig.7. Influence of the contact heat transfer coefficient B on the temperature ϑ at ξ=0, Λ=1 and Fo_0=10 (1-column image)

The analysis above shows that in general ϑ is sensitive to changes in the parameters Λ, Fo_0 and B.

5. Application range of the boundary conditions

The application range of the boundary conditions of Eq.(13) is estimated by investigating the heating of a semispace covered with a surface layer by a constant heat flux q_0. The schematic is presented in Fig.8a.

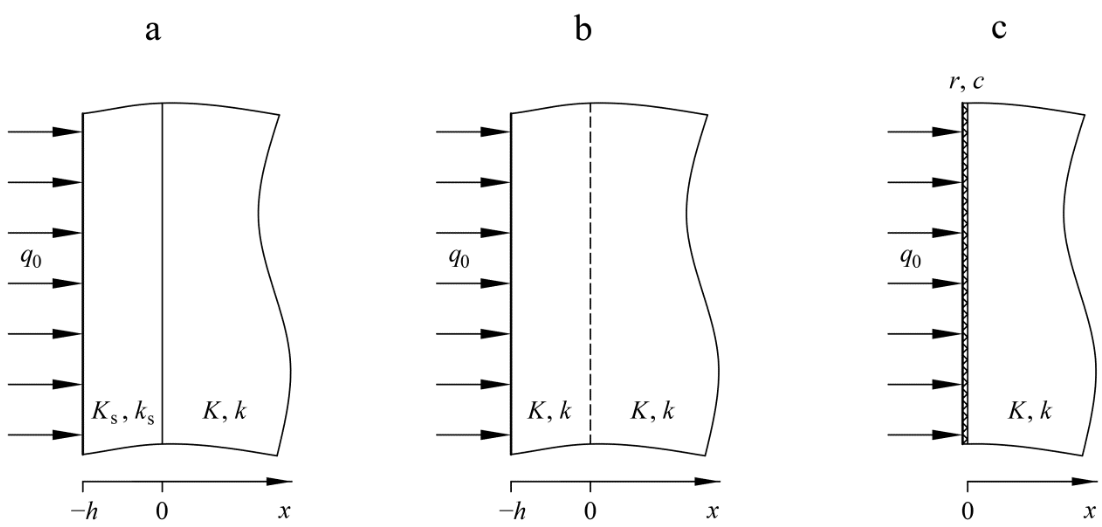

Fig.8. Schematics: (a) heating of a semispace with a surface layer; (b) heating of a semispace; (c) heating of a semispace due to Eq.(13) (2-column image)

The dimensionless temperature $\vartheta_e = KT/(q_0 h)$ at the boundary x=0 between the semispace and surface layer is derived from the exact solution obtained by Matysiak et al. [44]:

$$\vartheta_e(\mathrm{Fo}) = 4\sqrt{\mathrm{Fo}}\sum_{n=0}^{\infty}\frac{(\Lambda/\sqrt{\chi}-1)^n}{(\Lambda/\sqrt{\chi}+1)^{n+1}}\,\mathrm{ierfc}\left(\frac{2n+1}{2\sqrt{\chi\mathrm{Fo}}}\right) \tag{36}$$

where the integral of the error function (Carslaw and Jaeger [9], p.484)

$$\mathrm{ierfc}(z) = \frac{\exp\{-z^2\}}{\sqrt{\pi}} - \frac{2z}{\sqrt{\pi}}\int_z^{\infty}\exp\{-\tau^2\}\,d\tau$$

If the difference in the thermal properties of the surface layer and semispace is neglected, i.e. $\Lambda = \chi = 1$, as shown in Fig.8b, the dimensionless temperature ϑ_s at x=0 reads

$$\vartheta_s(\mathrm{Fo}) = 2\sqrt{\mathrm{Fo}}\,\mathrm{ierfc}\left(\frac{1}{2\sqrt{\mathrm{Fo}}}\right) \tag{37}$$

Replace the surface layer with a surface of equivalent thermal resistance $r = h/K_s$ and heat capacity $c = K_s h/k_s$, as shown in Fig.8c. This is tantamount to the specification of Eq.(13) at α=1, γ=0 and $q = q_0$. The dimensionless temperature ϑ_p at x=0 is easily obtained from Eq.(35) in the form

$$\vartheta_p(\mathrm{Fo}) = \frac{4}{\pi}\int_0^{\infty}\frac{(2-z^2/\chi)(1-\exp\{-z^2\mathrm{Fo}\})}{z^2((2\Lambda z/\chi)^2+(2-z^2/\chi)^2)}dz \tag{38}$$

Figure 9 illustrates the temperature curves ϑ_e, ϑ_s and ϑ_p obtained for Λ=0.1, i.e. when the surface layer has a 10 times smaller thermal conductivity K_s compared to K. It is clearly seen that ϑ_p tends to ϑ_e with increasing Fo, whereas the difference between ϑ_s and ϑ_e remains significant.

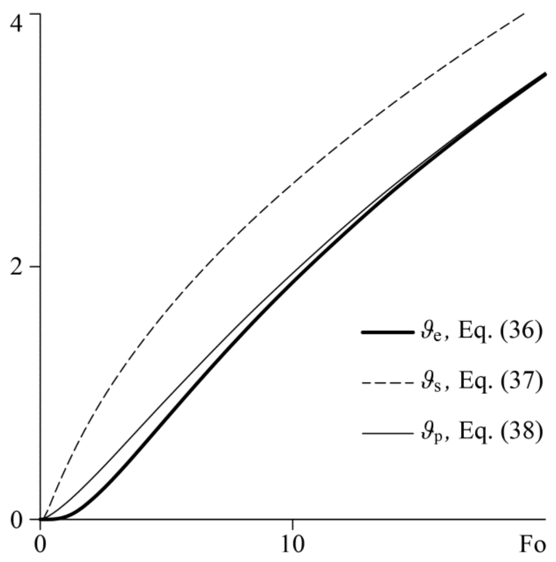

Fig.9. Comparison of the temperatures ϑ_e, ϑ_s and ϑ_p at Λ=0.1 (1-column image)

The error ε introduced by application of Eq.(13) is defined as the percent deviation of ϑ_{p} from ϑ_{e} for the sliding duration $\mathrm{Fo} = \mathrm{Fo}_0$:

$$\varepsilon = \left|1 - \frac{\vartheta_{\mathrm{p}}(\mathrm{Fo}_0)}{\vartheta_{\mathrm{e}}(\mathrm{Fo}_0)}\right| \cdot 100\%$$

Fig.10 shows contour lines of ε in the plane (Fo_0, Λ), along with the practical region estimated based on the data of Table 1. It is apparent that ε decreases with an increase in Fo_0 or Λ. ε is below 1% at Λ>0.19 for Fo_0=10 and already at Λ>0.011 for Fo_0=10^2. This trend is caused by that the temperature distribution in the surface layer becomes closer to linear, i.e. the assumption of Eq.(8) becomes more valid, with increasing sliding duration (t_0) or increasing surface layer thermal conductivity (K_{s}). The presented results suggest that application of Eq.(13) introduces a negligibly small error for a wide class of friction layers and coatings.

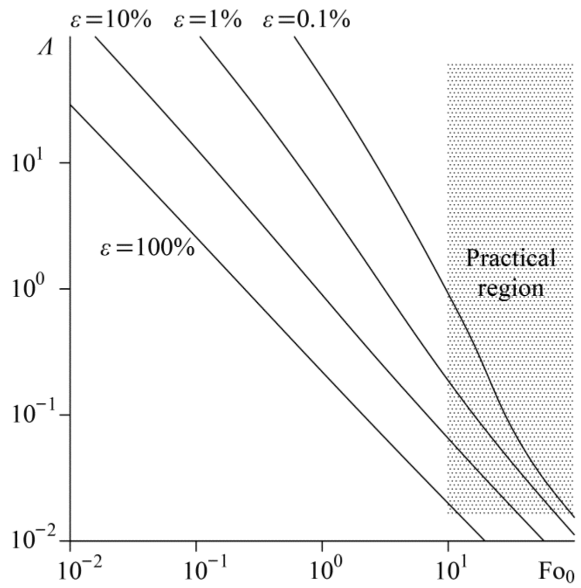

Fig.10. Dependence of the error ε on the sliding duration Fo_0 and thermal conductivity ratio Λ (1-column image)

Summarising the findings of the present study, it may be concluded that utilisation of the conditions of Eq.(13) allows simplifying the formulation and solution of thermal problems of sliding by eliminating surface layers from consideration without significant loss in accuracy. These conditions can be efficiently used for analytical studies and serve a basis for developing new numerical algorithms.

6. Conclusions

The proposed boundary conditions of Eq.(13) enable one to simplify essentially the solution of thermal problems of sliding in the presence of surface layers (friction layers and tribological coatings), characterising the surface layers by their thermal resistances and heat capacities. The analytical solution of Eq.(31) was derived for the problem of non-stationary heat conduction in two semispaces with the proposed conditions at their interface. It was shown that its particular cases coincide with the exact temperature expressions obtained for different well-known boundary conditions. Dimensionless analysis of the decelerative sliding of a semispace covered with a surface layer against a constant-temperature semispace revealed the temperature sensitivity to the surface layer thermal conductivity, sliding duration, and roughness contact heat transfer coefficient. It was found that the error introduced by the proposed conditions decreases with increasing sliding duration or increasing surface layer thermal conductivity. Review of the thermal properties of solid materials showed that the error does not exceed 1% for a wide class of friction layers and coatings.

This work was supported by the National Science Centre, Poland [grant number 2017/26/D/ST8/00142].

References

[1] J. Fourier, Théorie analytique de la chaleur, F. Didot, Paris, 1822. (in French)

[2] H.S. Carslaw, Introduction to the mathematical theory of the conduction of heat in solids, 2nd ed., Macmillan and Co., London, 1921.

[3] H. Blok, Theoretical study of temperature rise at surfaces of actual contact under oiliness lubricating conditions, General Discussion on Lubrication, Institution of Mechanical Engineers, London, 1937, vol.2, pp.222–235.

[4] J.C. Jaeger, Moving sources of heat and the temperature at sliding contacts, Proceedings of the Royal Society of New South Wales 76 (1942) 203–224.

[5] F. Charron, Partage de la chaleur entre ducs corps frottauts, Publ. scieut. et techn. Ministere air, 1943, no.182. (in French)

[6] J.F. Archard, The temperature of rubbing surfaces, Wear 2 (1958/59) 438–455.

[7] O. Nosko, Partition of friction heat between sliding semispaces due to adhesion-deformational heat generation, International Journal of Heat and Mass Transfer 64 (2013) 1189–1195.

[8] F.F. Ling, A quasi-iterative method for computing interface temperature distributions, Journal of Applied Mathematics and Physics 10 (1959) 461–474.

[9] H.S. Carslaw, J.C. Jaeger, Conduction of heat in solids, 2nd ed., Oxford University Press, London, 1959.

[10] A. Cameron, A.N. Gordon, G.T. Symm, Contact temperatures in rolling/sliding surfaces, Proceedings of the Royal Society A 286 (1965) 45–61.

[11] Ya.S. Podstrigach, The temperature field in a system of rigid bodies coupled by thin interface, Journal of Engineering Physics and Thermophysics 6 (10) (1963) 129–136. (in Russian)

[12] W.A. Mersman, Heat conduction in an infinite composite solid with an interface resistance, Transactions of the American Mathematical Society 53 (1) (1943) 14−24.

[13] J.R. Barber, The conduction of heat from sliding solids, International Journal of Heat and Mass Transfer 13 (1970) 857–869.

[14] G.A. Berry, J.R. Barber, The division of frictional heat — a guide to the nature of sliding contact, Journal of Tribology 106 (1984) 405–415.

[15] B.V. Protasov, Energy proportions in a tribosystem and prognostication of its service durability, Saratov University Publisher, Saratov, 1979. (in Russian)

[16] J.P. Bardon, Bases physiques des conditions de contact termique imparfait entre milieux en glissement relatif, Revue Générale de Thermique 386 (1994) 85–92. (in French)

[17] N. Laraqi, Phénomène de constriction thermique dans les contacts glissants, International Journal of Heat and Mass Transfer 39 (1996) 3717–3724. (in French)

[18] P. Chantrenne, M. Raynaud, Study of a macroscopic sliding contact thermal model from microscopic models, International Journal of Thermal Sciences 40 (2001) 603–621.

[19] S.A. Schaaf, On the superposition of a heat source and contact resistance, Quarterly of Applied Mathematics 5 (1) (1947) 107–111.

[20] G.T. Symm, Surface temperatures of two rubbing bodies, The Quarterly Journal of Mechanics and Applied Mathematics 20 (3) (1967) 381–391.

[21] J. Bos, H. Moes, Frictional heating of tribological contacts, Journal of Tribology 117 (1995) 171–177.

[22] B. Li, P.C. Clapp, J.A. Rifkin, X.M. Zhang, Molecular dynamics calculation of heat dissipation during sliding friction, International Journal of Heat and Mass Transfer 46 (2003) 37–43.

[23] K. Chen, L. Wang, Y. Chen, Q. Wang, Molecular dynamics simulation of microstructure evolution and heat dissipation of nanoscale friction, International Journal of Heat and Mass Transfer 109 (2017) 293–301.

[24] M. Eriksson, S. Jacobson, Tribological surfaces of organic brake pads, Tribology International 33 (2000) 817–827.

[25] P. Filip, Z. Weiss, D. Rafaja, On friction layer formation in polymer matrix composite materials for brake applications, Wear 252 (2002) 189–198.

[26] H. So, D.S. Yu, C.Y. Chuang, Formation and wear mechanism of tribo-oxides and the regime of oxidational wear of steel, Wear 253 (2002) 1004–1015.

[27] T. Akiyama, H. Ohta, R. Takahashi, Y. Waseda, J. Yagi, Measurement and modeling of thermal conductivity for dense iron oxide and porous iron ore agglomerates in stepwise reduction, ISIJ International 32 (7) (1992) 829–837.

[28] A. Loizou, H.S. Qi, A.J. Day, Analysis of heat partition ratio in vehicle braking processes, Braking 2009, St William's College, York, 2009.

[29] G. Straffelini, S. Verlinski, P.C. Verma, G. Valota, S. Gialanella, Wear and contact temperature evolution in pin-on-disc tribotesting of low-metallic friction material sliding against pearlitic cast iron, Tribology Letters 62 (2016) 36.

[30] K. Holmberg, H. Ronkainen, A. Matthews, Tribology of thin coatings, Ceramics International 26 (2000) 787−795.

[31] S. Hogmark, S. Jacobson, M. Larsson, Design and evaluation of tribological coatings, Wear 246 (2000) 20–33.

[32] C. Donnet, A. Erdemir, Historical developments and new trends in tribological and solid lubricant coatings, Surface and Coatings Technology 180–181 (2004) 76–84.

[33] M.V. Kindrachuk, Yu.Ya. Dushek, M.V. Luchka, A.N. Gladchenko, Evolution of the structure and properties of eutectic coatings during friction, Poroshkovaya Metallurgiya (5–6) (1995) 104–110.

[34] Y.S. Touloukian, R.W. Powell, C.Y. Ho, P.G. Klemens, Thermophysical properties of matter. Volume 2. Thermal conductivity: Nonmetallic solids, IFI/Plenum, New York, 1970.

[35] Y.S. Touloukian, R.W. Powell, C.Y. Ho, P.G. Klemens, Thermophysical properties of matter. Volume 1. Thermal conductivity: Metallic elements and alloys, IFI/Plenum, New York, 1970.

[36] V.A. Shevchuk, Calculation of thermal state of bodies with multilayer coatings, International Conference on Computational Science 2002. Lecture Notes in Computer Science, Springer, Berlin, 2002, vol.2330, pp.500–509.

[37] Ya.S. Podstrigach, P.R. Shevchuk, Effect of surface layers on diffusion processes and the resulting stress state in solids, Soviet Materials Science 3 (5) (1968) 420–426.

[38] V.A. Shevchuk, Generalized boundary conditions for heat transfer between a body and the surrounding medium through a multilayer thin covering, Journal of Mathematical Sciences 81 (6) (1996) 3099–3102.

[39] A.L. Nosko, N.S. Belyakov, A.P. Nosko, Application of the generalized boundary condition to solving thermal friction problems, Journal of Friction and Wear 30 (6) (2009) 455–462.

[40] J.H. Lienhard IV, J.H. Lienhard V, A heat transfer textbook, 4th ed., Phlogiston Press, Cambridge (U.S.A.), 2017.

[41] D.V. Grilitskii, Thermoelastic contact problems in tribology, The Institute of Topics and Methods of Teaching, Kyiv, 1996. (in Ukrainian)

[42] P.P. Krasnyuk, Quasistatic contact interaction of two layers with heat generation caused by friction, Materials Science 35 (2) (1999) 180−192.

[43] S.J. Matysiak, A.A. Yevtushenko, E.G. Ivanyk, Contact temperature and wear of composite friction elements during braking, International Journal of Heat and Mass Transfer 45 (2002) 193–199.

[44] S. Matysiak, A. Evtushenko, M. Kutsei, Non-stationary heating of a uniform foundation coated with a surface composite layer, Journal of Friction and Wear 25 (6) (2004) 11–18.

[45] Yu.O. Pyr’ev, Investigation of the contact interaction between two layers with regard for the temperature dependence of friction and wear coefficients, Journal of Mathematical Sciences 109 (1) (2002) 1257–1265.

[46] F. de Monte, An analytic approach to the unsteady heat conduction processes in one-dimensional composite media, International Journal of Heat and Mass Transfer 45 (2002) 1333–1343.

[47] A. Evtushenko, M. Kutsey, Effect of external surface cooling of the plane-parallel layer on the temperature of the layer–base tribosystem, Journal of Friction and Wear 29 (6) (2008) 455–460.

[48] A.A. Yevtushenko, M. Kuciej, Influence of the convective cooling and the thermal resistance on the temperature of the pad/disc tribosystem, International Communications in Heat and Mass Transfer 37 (2010) 337–342.

[49] A. Yevtushenko, M. Kuciej, Two heat conduction problems with frictional heating during braking, Journal of Theoretical and Applied Mechanics 48 (2) (2010) 367−380.

[50] A.A. Yevtushenko, M. Kuciej, The thermal problem of friction for a three-element tribosystem with composite strip, International Journal of Heat and Mass Transfer 54 (2011) 5427–5437.

[51] N.S. Belyakov, A.P. Nosko, Mathematical simulation of thermal friction processes under conditions of nonideal contact, High Temperature 47 (1) (2009) 123–130.

[52] N.S. Belyakov, A.P. Nosko, Thermoelastic problem of friction of plane-parallel layers with allowance for nonstationarity of thermal processes, Journal of Friction and Wear 31 (5) (2010) 317−325.

[53] N. Belyakov, O. Nosko, Analytical solution of non-stationary heat conduction problem for two sliding layers with time-dependent friction conditions, International Journal of Heat and Mass Transfer 98 (2016) 624−630.

[54] I. Dülk, T. Kovácsházy, Steady-state heat conduction in multilayer bodies: An analytical solution and simplification of the eigenvalue problem, International Journal of Heat and Mass Transfer 67 (2013) 784–797.

[55] Y.S. Touloukian, E.H. Buyco, Thermophysical properties of matter. Volume 4. Specific heat: Metallic elements and alloys, IFI/Plenum, New York, 1970.

[56] Y.S. Touloukian, E.H. Buyco, Thermophysical properties of matter. Volume 5. Specific heat: Nonmetallic solids, IFI/Plenum, New York, 1970.